Available online at www.sciencedirect.com
SCIENCE DIRECT®
Journal of Molecular Catalysis A: Chemical 234 (2005) 169–179
JOURNAL OF MOLECULAR CATALYSIS A: CHEMICAL
www.elsevier.com/locate/molcata

X-ray absorption near edge structure and X-ray photo electron spectroscopy analyses of $NiMo/Al_2O_3$ catalysts containing boron and phosphorus

D. Ferdous [a], A.K. Dalai [a,*], J. Adjaye [b]

[a] *Catalysis and Chemical Reactor Engineering Laboratories, Department of Chemical Engineering, University of Saskatchewan, 110 Science Place, Saskatoon, SK, Canada S7N 5C9*
[b] *Syncrude Canada Ltd., Edmonton Research Center, Canada*

Received 4 January 2005; received in revised form 1 March 2005; accepted 1 March 2005

Abstract

In this work, three catalysts namely $NiMo/Al_2O_3$, $NiMoB/Al_2O_3$, $NiMoP/Al_2O_3$ were prepared and surface structure studied using X-ray absorption fine structure (EXAFS), X-ray absorption near edge structure (XANES) and X-ray photo electron spectroscopy (XPS). In the boron and phosphorus containing catalysts, boron and phosphorus concentrations were maintained at 1.7 and 2.7 wt.%, respectively. The surface structure of the catalysts at different stages of reactions (after 1 and 2 days of sulfidation, after 1 and 5 days of precoking and after 30 days of run time) was studied. Results from EXAFS analysis indicated the presence of similar P─O bond distance in all phosphorus containing samples. XPS and S K-edge spectra obtained from XANES showed the presence of two oxidation states of sulfur such as −2 and +6. Boron and phosphorus significantly increased the sulfidity of the catalyst, confirmed from XPS analysis. These catalysts showed less carbon deposition during hydrotreating process. Ni and Mo dispersion also increased significantly with the incorporation of boron in $NiMo/Al_2O_3$ catalyst, thus increasing the extent of hydrotreating reactions.

Keywords: Hydrodenitrogenation; Hydrodesulfurization; Promoters; Surface Structure; EXAFS; XANES; XPS

1. Introduction

Hydrotreating catalysts have played an important role in producing cleaner fuels by removing heteroatoms and saturating aromatic compounds [1]. For many years, nickel or cobalt promoted catalysts containing molybdenum and tungsten have been used in hydrotreating, which may include hydrodesulphurization (HDS), hydrodenitrogenation (HDN), hydrodeoxygenation (HDO), and hydrodemetallization (HDM). However, when these catalysts are applied in hydrotreating of heavy gas oils derived from bitumen, the effectiveness for removal of heteroatoms such as sulfur, nitrogen or oxygen, is drastically reduced.

An important step in the formulation and design of a better catalyst is to establish a structure-activity relationship. A better description of Co(Ni)MoS phases presents a huge interest for improving the preparation, activation and usage of hydrotreating catalysts for industrial refining [2]. The catalyst structure is a combination of the physical, chemical and morphological properties. The definition of catalyst structure is not trivial [3]. Detailed structural information related to hydrotreating catalysts, which consist mostly of alumina-supported Co(Ni) promoted MoS_2, is difficult to obtain because of their structural complexity [4].

Literature indicates that morphological and structural effects have significance for the number of active sites in hydrotreating catalyst, as suggested by Kasztelan and co workers [5–7]. Their work shows that it is possible to establish quantitatively relationships between HDS activity and the

* Corresponding author. Tel.: +1 306 966 4771; fax: +1 306 966 4777.
E-mail address: ajay.dalai@usask.ca (A.K. Dalai).

1381-1169/$ – see front matter © 2005 Elsevier B.V. All rights reserved.
doi:10.1016/j.molcata.2005.03.004

number and type of active sites (MoS_2). As a consequence, the controlling MoS_2 means the controlling the nature of the exposed active sites and thus, the reactivity [2].

There are number of analytical techniques used to characterize the structure including the sulfide phase of the catalyst. These methods include X-ray photoelectron spectroscopy (XPS), Mössbauer emission spectroscopy (MES), the extended X-ray absorption fine structure (EXAFS) and high resolution transmission electron microscopy (HRTEM).

X-ray photoelectron spectroscopy (XPS) has been used successfully in the past to characterize both Co–Mo/Al_2O_3 and NiMo/Al_2O_3 catalysts [8–12]. Alstrup et al. [10] used this technique to measure the binding energy (BE) of different components on the Co–Mo/Al_2O_3 catalyst surface.

The local structure of Mo and Ni in typical sulfided alumina supported NiMo catalysts have been studied by different authors. A coordination of six sulfur atoms around molybdenum on the sulfide catalyst was reported from EXAFS analysis using well chosen reference materials (NiO, $NiMoO_4$, MoO_3, MoS_2) extracting parameters for phase shift and scattering amplitude [13].

Burch and Collins [14] from the O_2 and CO uptakes estimated the average size of the MoS_2 particles corresponding to about 33 Mo atoms (i.e. 1.5–2.0 nm in basal plan direction) on a sulfided Mo/Al_2O_3 catalyst. This value is somewhat larger than the typical values estimated from EXAFS. Rodriguez et al. [15] studied the oxidation states of sulfur present in sulfided cobalt and nickel molybdates using S K-edge XANES. They concluded that there are at least two types of sulfur species present on this type of catalyst. One associated with a formal oxidation state of −2 (MoS_2, CoS_x or NiS_x) and the other associated with a formal oxidation state of +6 (SO_4^{2-}).

Cattaneo et al. [16] investigated the sulfidation of Mo and Ni in SiO_2-supported NiMo hydrotreating catalyst using quick EXAFS. They concluded that the sulfidation of Mo takes place in four regions. The first region is the temperature range in which molybdenum is present in the oxidic form. The two intermediate regions were observed during the sulfidation of molybdenum, the first consisting of molybdenum oxysulfides and the second of a pure Mo(IV)-S product. Their results showed that sulfidation of nickel occur in a smaller temperature range in comparison with the sulfidation of Mo.

Cattaneo et al. [17] used in situ EXAFS technique in order to study the influence of chelating ligands on the HDN and HDS activities of γ-Al_2O_3-supported NiMo catalyst. From K-edge quick EXAFS and normal EXAFS data they concluded that the highest HDN activity was obtained at the lowest temperature and with the highest structural order of MoS_2 crystallites. The QEXAFS data indicated that a MoS_3-like phase preceded MoS_2 during the sulfidation process.

Pettiti et al. [18] also used in situ EXAFS technique to characterize the Mo, Co and Ni sulfided phase supported on γ-Al_2O_3. They concluded that Co and Mo metals occupied six-fold sites in the CoMo γ-Al_2O_3 whereas Mo was octahedrally coordinated in the NiMo/γ-Al_2O_3 and that in-situ EXAFS analysis is a better tool to interpret the relationship between the surface properties of the catalyst with the HDN and HDS activities.

Although CoMo/Al_2O_3 and NiMo/Al_2O_3 and related catalysts have been used commercially for more than 70 years, the exact chemical nature, structure and shape of the active species are still not known. Also, this type of catalyst goes through different structural and morphological changes from sulfidation to 30 days of run time. Information on structural changes with time is very limited in literature. In the present work, a systematic study has been performed to study the surface structure of boron and phosphorus containing catalyst at different stages of the reaction for the hydrotreating of heavy gas oil derived from Athabasca bitumen.

2. Experimental

2.1. Catalyst preparation

In this work, three catalysts namely NiMo/Al_2O_3, NiMoB/Al_2O_3 and NiMoP/Al_2O_3 were prepared using incipient wetness coimpregnation method. In this method, an ammoniacal solution (28 wt.% concentrated NH_3) was prepared using required amount of ammonium heptamolybdate [$(NH_4)_6Mo_7O_{24}{\cdot}4H_2O$] and nickel nitrate [$Ni(NO_3)_2{\cdot}6H_2O$]. NiMoB/$Al_2O_3$ catalysts were prepared by impregnating appropriate solutions of boric acid (H_3BO_3) on to a NiMo/Al_2O_3 catalyst. NiMoP/Al_2O_3 catalyst was prepared using incipient wetness coimpregnation method. In this case, a solution containing required amount of ammonium heptamolybdate [$(NH_4)_6Mo_7O_{24}{\cdot}4H_2O$], nickel nitrate [$Ni(NO_3)_2{\cdot}6H_2O$] and phosphoric acid ($H_3PO_4$) in water was impregnated onto an Al_2O_3 support. The detail preparation procedures are given elsewhere [19].

2.2. Surface structure studies

Catalyst samples listed in Table 1 were collected at different stages of the reaction in order to study the surface structure. All the experiments were performed at typical hydrotreating process conditions in a micro scale trickle bed reactor using 5 mL of catalyst in each case using heavy gas oil derived from Athabasca bitumen. The temperature, total pressure, liquid hourly space velocity (LHSV), and H_2/Feed ratio were maintained at 385 °C, 1275 psig, 1 h^{-1} and 600 mL/mL, respectively. The detail procedures are given elsewhere [20].

All catalysts were cleaned before performing surface structure studies. For cleaning, catalysts were soaked in toluene (Aldrich, 99.5%) for 3 h and cleaned again with toluene four or five times. Cleaned catalysts were then dried in an oven overnight at 150 °C. The surface structure and morphology of the catalyst were studied using extended X-ray ab-

Table 1
List of catalyst used for surface structure studies

Catalyst type	Stages of reaction
(1) Catalyst-B–Ni (3 wt.%) Mo (14 wt.%)/Al_2O_3 calcined at 500 °C	(1) After 1 day of sulfidation (2) After 2 days of sulfidation (3) After 1 day on stream (4) After 5 days on stream (5) After 30 days run
(2) Catalyst-M–Ni (3 wt.%) Mo (14 wt.%) B (1.7 wt.%)/Al_2O_3	(1) After 1 day of sulfidation (2) After 2 days of sulfidation (3) After 1 day on stream (4) After 5 days on stream (5) After 30 days run
(3) Catalyst-N–Ni (3 wt.%) Mo (14 wt.%) P (2.7 wt.%)/Al_2O_3	(1)After 1 day of sulfidation (2) After 2 days of sulfidation (3) After 1 day on stream (4) After 5 days on stream (5) After 30 days run

sorption fine structure (EXAFS), X-ray absorption near edge structure (XANES) and X-ray photo electron spectroscopy (XPS) analyses. The detail descriptions of these analyses are given below.

2.2.1. Extended X-ray absorption fine structure and X-ray absorption near edge structure

Extended X-ray absorption fine structure (EXAFS) and X-ray absorption near edge structure (XANES) of all catalysts listed in Table 1 were performed at the Synchrotron Radiation Centre (CRC), Madison, WI in order to study the oxidation structure of S, B and P. Also, different phases present in the catalyst containing phosphorus at different stages of reaction were examined. The measurements were carried out in fluorescence yield mode on the Canadian Double Crystal Monochromator (DCM) and Canadian Grasshopper Monochromator (GM) beam lines. For both kinds of measurement, catalyst samples were pressed into self supported wafers and then put into soft X-ray beam. P K-edge EXAFS was performed using Canadian DCM beam line. S and P K-edge XANES analysis of all catalysts were performed for the energy range of 2460–2520 eV and 2140–2200 eV, respectively using Canadian DCM beam line. B K-edge XANES analysis of all catalysts containing boron was performed for the energy range of 180–225 eV using Canadian GM. In all cases the spectra around the edge jump, were fitted by a linear function of standard compounds. Standard procedures were used to extract the EXAFS data from the absorption spectra using WINXAS software. The peaks obtained from S, P and B K-edge XANES were identified using standard samples such as MoS_2, Na_3PO_4 and borax ($Na_2B_4O_7{\cdot}10H_2O$), respectively.

The collected P K-edge EXAFS data were averaged and k_1 weighted EXAFS functions were Fourier Transformed.

2.2.2. X-ray photo electron spectroscopy

X-ray photo electron spectroscopy analysis of all catalyst samples listed in Table 1 was performed using Kratos Axis Ultra XPS equipment using monochromated Al Kα X-ray radiation. The pressure of the analysis chamber was maintained at 4×10^{-8} Torr. For each sample, two particles were analyzed and the average data for the peak area and binding energy (BE) was taken. During XPS analysis, there was no indication of charging. The carbon 1S binding energy of 285 eV was used as a reference for determining the binding energies.

3. Results and discussion

Our previous studies indicated that the addition of boron and phosphorus to NiMo/Al_2O_3 caused a significant increase in HDN of heavy gas oil derived from Athabasca bitumen. For example, the total nitrogen conversion increased from 62.0 to 78.0 wt.% with the incorporation of 1.7 wt.% boron to NiMo/Al_2O_3 when the experiment was performed at the temperature, pressure, LHSV and H_2/feed ratio of 385 °C, 8.7 MPa, 1 h^{-1} and 600 mL/mL, respectively (see Fig. 1). On the other hand, total nitrogen conversion also increased from 62.0 to 78.4 wt.% with the incorporation of 2.7 wt.% phosphorus to NiMo/Al_2O_3 at the same operating conditions. So, it is important to study the effect of boron and phosphorus on the structure of the catalysts to understand the mechanism of HDN and HDS reactions and deactivation process using this catalyst. In this work, the surface structure of catalyst containing boron and phosphorus was studied at different stages of reactions using extended X-ray absorption fine structure (EXAFS), X-ray absorption near edge structure (XANES) and X-ray photo electron spectroscopy (XPS). For these studies, it was assumed that exposure to air during sample cleaning and sample preparation has very negligible effect on the surface structure and morphology of these catalysts [21]. The detail discussion on these analyses is given below.

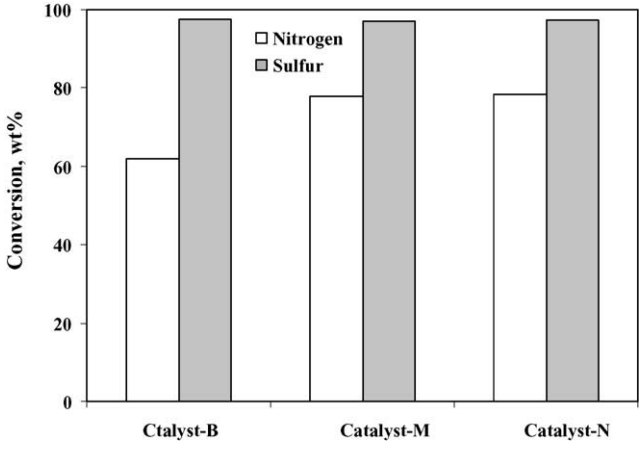

Fig. 1. Nitrogen and sulfur conversions of heavy gas oil derived from Athabasca bitumen using catalysts- B, M and N at the temperature, pressure, LHSV and H_2/feed ration of 385 °C, 8.7 MPa, 1 h^{-1} and 600 mL/mL, respectively.

3.1. P K-edge extended X-ray absorption fine structure

P K-edge X-ray absorption fine structure (EXAFS) analysis was performed in order to study the local environment of P (P–O bond length and P–O coordination) in catalyst-N at different stages of hydrotreating reaction such as after 1 and 2 days of sulfidation, after 1 and 5 days on stream and after 30 days of run time. P K-edge EXAFS for the reference compound (Na_3PO_4) was also performed. The absorption spectra were obtained by averaging 5–15 experimental spectra. From the Fourier transform (FT) plot of Na_3PO_4, a major peak in the range of 0.3–1.6 Å was observed. This peak corresponds to the four O atoms constituting the PO_4 tetrahedron [22]. The presence of PO_4 was confirmed from the P K-edge XANES analysis. The interpretations of the peaks in the range of 1.6–6 Å were not attempted. A peak in the range of 0–0.3 Å is due to the background noise. Similar trends were also observed for all catalyst samples. The distribution region and amplitude for the peak in the range of 0.3–1.6 Å were the same for all catalyst samples indicating that the atoms in this coordination shell may have similar distance relative to the central absorbing phosphorus. Furthermore, the coordination number may also be similar because of the similar peak amplitude. These facts show that the phosphorus-coordination environment may be similar among these samples. Samples also carry some fine structures, which are attributed to the noise of the collected data. From Fourier transform, it was observed that, the peak intensity for the reference sample obtained in the range of 0.3–1.6 Å was significantly lower than those from catalyst samples, probably due to differences in the phosphorus concentrations, which caused self absorption in fluorescence detection and left lower apparent XAFS amplitude.

From $k\chi(k)$ (k weighted fine structure), spectra was analyzed for the reference as well as for the catalyst samples. The k weighting of 1 makes the spectral oscillations relatively uniform amplitude in the low and high k region. The oscillation frequency and amplitude of the $k\chi(k)$ spectra for all catalyst samples were the same but were somewhat different for the reference sample. From the comparison of oscillation frequency and amplitude of the $k\chi(k)$ spectra and FT magnitude, it can be concluded that the chemistry and phosphorus coordination environment in the reference compound are different from those for the catalyst samples.

3.2. X-ray absorption near edge structure

X-ray absorption near edge structure (XANES) was used to study the bulk oxidation states of S, B and P present in catalysts-B, M, N at different stages of reactions. It should be mentioned that XANES data was not normalized. The results obtained from S, B and P K-edge XANES analysis are described below.

3.2.1. S K-edge X-ray absorption near edge structure

XANES performed with synchrotron radiation has emerged as a very powerful tool for characterizing the electronic properties of catalytic materials [23]. An S K-edge XANES analysis of different $NiMo/Al_2O_3$ catalysts containing boron and phosphorus was performed using synchrotron radiation.

The S K-edge spectra of $NiMo/Al_2O_3$ (catalyst-B) at different stages of reactions, as well as model MoS_2, are given in Fig. 2a. The S K-edge spectra of MoS_2 can be characterized by a sharp edge peak at 2476 eV followed by two additional peaks at 2483 and 2493 eV. On the other hand, the S K-edge spectra of sulfided $NiMo/Al_2O_3$ catalyst can be characterized by two peaks at 2476 and 2484 eV. This indicates the presence of two oxidation states of sulfur for sulfided $NiMo/Al_2O_3$ catalyst. The sulfur appearing at the photon energy of 2476 eV (oxidation state ~ -2) is associated with the presence of metal-sulfur bonds (MoS_2 and NiS_x), whereas the sulfur at 2484 eV (oxidation state +6) is associated with the presence of sulphate species (SO_4^{2-}), formed because of the oxidation of sulfur in the presence of oxygen of the molybdates [15]. SO_4^{2-} can also be formed because of the minor oxidation of S^{2-} in presence of air during sample preparation [21]. Similar results were also observed by Rodriguez et al. [15] and Chaturvedi et al. [24] for the sulfided α-$NiMoO_4$ and sulfided β-$NiMoO_4$ catalyst.

From Fig. 2a it is also observed that the intensity of these two peaks increased with the increase in the extent of sulfidation. It is also evident from this figure that the intensity of the peak at 2476 eV remained constant for catalyst-B during the rest of the reaction. But the intensity of peak at 2484 eV slightly increased with the increase in TOS. It is observed that sulfidation of this catalyst not only forms MoS_2, considered as the active phase of this catalyst but also forms SO_4, which can be considered as an undesired species for hydrotreating reactions.

The effect of boron on the oxidation states of S is given in Fig. 2b. This figure also shows similar two peaks as in case of catalyst without boron. From this figure it is observed that the peak intensity increased with the increase in the extent of sulfidation, whereas the stabilization of the catalyst decreased the peak intensity at 2484 eV. After 5 days on stream the peak intensity was diminished. This is probably due to the reduction of sulfate in the presence of hydrogen. This indicates that the presence of boron hinders the oxidation of elemental sulfur which forms during the sulfidation reaction and most of the sulfur takes part in the reaction to form H_2S. From the comparison of Fig. 2a and b, it is observed that catalyst-B after sulfidation had a higher concentration of $-SO_4^{2-}$ than that for catalyst-M. It can also be concluded from these two figures that the $-SO_4^{2-}$ formed during the sulfidation of catalyst without boron (catalyst-B) are less reducible and different in nature from those formed during the sulfidation of catalyst with boron (catalyst-M). It is also evident from the Fig. 2a and b that the formation of MoS_2 and SO_4^{2-} for the catalyst containing boron are lower than those obtained from catalyst without boron after 1 day of sulfidation.

The effect of phosphorus on the oxidation state of sulfur is given in Fig. 2c. This figure also shows a similar trend

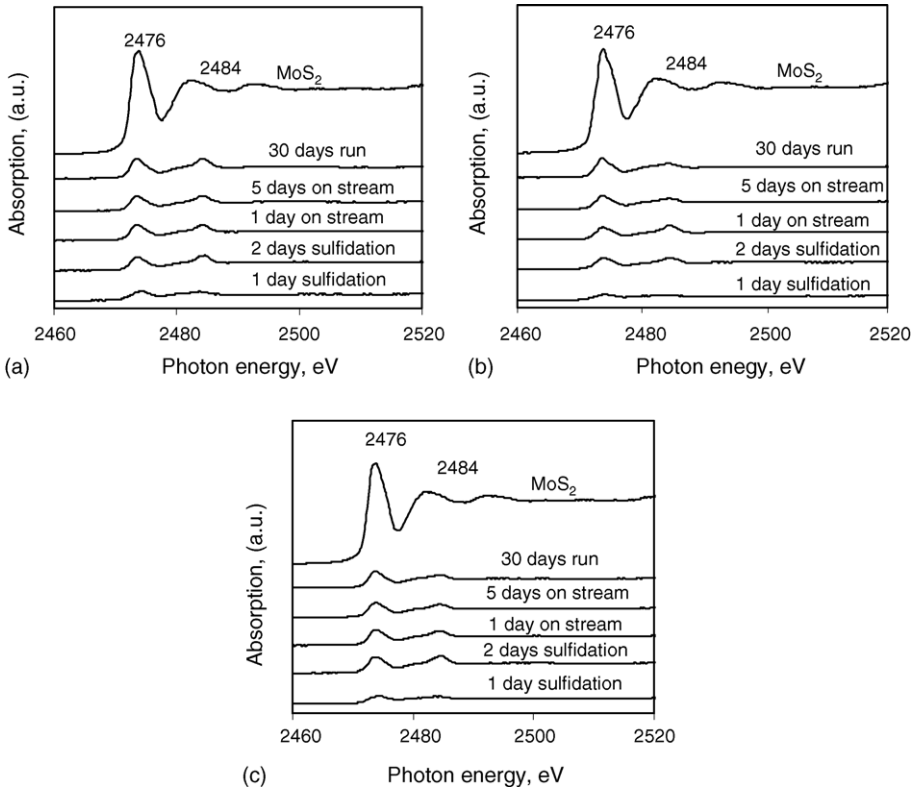

Fig. 2. S K-edge XANES spectra of different catalysts at different stages of reactions (a) catalyst-B; (b) catalyst-M and (c) catalyst-N.

as in Fig. 2b. The peak intensity for the presence of SO_4^{2-} decreased after the stabilization of this catalyst, however, is slightly higher than that for catalyst-M. Furthermore, from Fig. 2a, b, and c, it is seen that the peak intensity for the formation MoS_2 for the catalyst containing boron and phosphorus (catalysts- M and N) is comparable with that from catalyst-B.

3.2.2. B K-edge X-ray absorption near edge structure

B K-edge XANES of catalyst containing boron was performed to obtain the oxidation states of boron for the catalyst sample collected at different stages of reactions. The B K-edge XANES spectra strongly reflect the local structure around boron atoms [25,26]. The B K-edge spectra for catalyst-M and for a model compound (borax) are given in Fig. 3. XANES of borax are characterized by the sharp peak at the energy of 194 eV and a diffused peak at the energy of 199 eV. The sharp peak is assigned to the transition of B 1s electrons to the unoccupied B $2p_z$ state (π^*) which indicates that boron is trigonally coordinated with oxygen. The diffused peak at 199 eV is assigned to the transition of B 1s electrons to unoccupied sigma antibonding (σ^*) states of BO_4 group [27]. This BO_4 is responsible for an increase in acidity of catalyst-M [28]. From this figure it is observed that all catalyst samples have only one peak at the energy of 194 eV, which indicates that these samples contain trigonally coordinated B, most likely due to B_2O_3 [29]. It is also observed that after sulfidation and stabilization of the catalyst, B_2O_3 remained in the catalyst and its intensity did not change with the increase in TOS. This present study did not show any evidence of presence of BO_4, which agreed with Li et al. [29] for the fresh $NiMo/Al_2O_3–B_2O_3$ catalyst.

3.2.3. P K-edge X-ray absorption near edge structure

P K-edge XANES was performed in order to study the oxidation state of phosphorus in catalyst-N at different stages of reactions. The P K-edge spectra for this catalyst as well as the model compound (Na_3PO_4) are given in Fig. 4. The XANES spectra for the model compound can be characterized by three peaks at 2156, 2165, and 2173 eV, respectively.

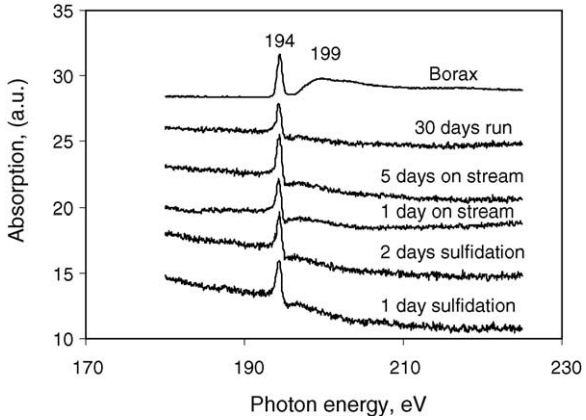

Fig. 3. B K-edge XANES spectra of catalyst-M at different stages of reactions.

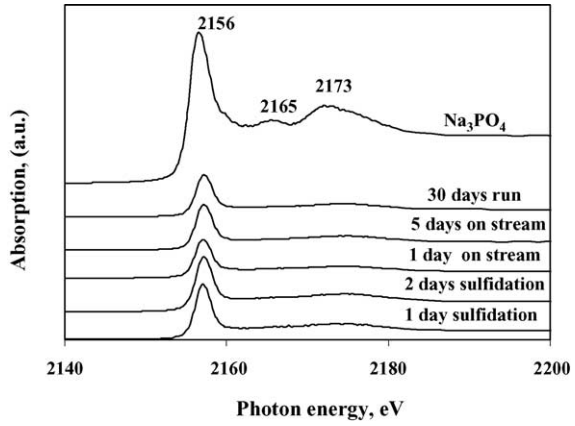

Fig. 4. P K-edge XANES spectra of catalyst-N at different stages of reactions.

The peak at 2156 eV can be attributed to the tetrahedrally coordinated phosphorus [30]. Since the PO_4 group has T_d symmetry this peak is assigned to a transition of the P 1s electron into an unoccupied valence electronic state formed by the overlap of P sp^3 hybrid and O 2p-orbitals [30,31]. Peaks at 2165 and 2173 eV can be attributed to the P–O–P and P–O bridges in the catalyst [30]. From this figure it is observed that all samples give one large peak at 2156 eV which matches with the first peak of the model compound which indicates that phosphorus in the catalyst is present in the form of PO_4. A diffused peak at 2173 eV was observed after 1 day of sulfidation which is attributed to the formation of a P–O bridge in the catalyst sample but it diminished with the increase in TOS. In catalyst-N, a P–O–P bridge was not observed (see Fig. 4). From this figure it is also observed that there is no change in peak intensity at 2156 eV after 1 and 2 days of sulfidation which indicates that phosphorus remains in the form of PO_4 after sulfidation of the catalyst. However, the peak intensity slightly decreased after 1 and 5 days on stream. It is probably due to the reduction of PO_4 on $NiMo/Al_2O_3$ catalyst in the presence of hydrogen and other compounds present in the feed material. However, in case of $NiMoP/SiO_2$ the reduction of phosphate only occurs in the temperature range of 600–800 °C [32].

3.3. X-ray photo electron spectroscopy

X-ray photo electron microscopy (XPS) analysis of catalysts- B, M and N obtained at different stages of reactions was carried out in order to study the surface carbon deposition and surface structure such as the dispersion of Ni and Mo and to confirm the oxidation states of S, Ni and Mo on the catalyst surface. The detail results are discussed below.

3.3.1. Carbon deposition

Coke deposition on the catalyst is generally believed to be the primary cause of catalyst deactivation in hydrotreating different petroleum distillates [33]. The deactivation is a complex process that may involve several different routes with different intermediates and mechanisms [34]. It is believed that coke deposition is the consequence of a polymerization/hydrogenation reaction which generates coke structures capable of physically impeding the access of reagents to active centers and progressively blocking the porous structure of the catalyst [35]. Therefore, it is necessary to study the carbon deposition at different stages of reactions to correlate which stages are responsible for maximum carbon deposition on the catalyst and hence catalyst deactivation.

The percentage of carbon deposition at different stages of the reaction is given in Table 2. From this table it is observed that the carbon deposition on the catalyst surface increased significantly with the increase in TOS. For catalyst-B the deposition of carbon increased from 22.6 to 44.1 at.% after 30 days of run time. The increase in carbon deposition during sulfidation is probably due to the cracking of different hydrocarbons formed from butanethiol ($C_4H_{10}S$) during the sulfidation reaction. It is evident from this table that the rate of carbon deposition decreased with the increase in time on stream. For example, when the heavy gas oil was used the deposition of carbon increased from 28.3 to 35.4 at.% after 24 h of run time. At the end of 5 and 30 days on stream the carbon deposition increased from 35.4 to 39.6 at.% and then to 44.1 at.%. Zhang et al. [36] also reported significant carbon deposition on the $NiMo/Al_2O_3$ catalyst surface after 1000 h of run tine, however did not quantify the amount. Marafi and Stanislaus [37] showed a rapid coke build-up on the catalyst surface as soon as the feed was introduced, reached as high as 10 wt.% within 3 h and reached at an equilibrium value within 24 h.

The change in carbon deposition on catalyst-M (containing boron) at different stages of the reaction is also given in Table 2. This table shows different trends from that of catalyst-B. No change in carbon deposition was observed after 2 days of sulfidation but it increased significantly after introducing heavy gas oil. For catalyst-M, the rate of carbon deposition during stabilization was higher than that on catalyst-B. For example, the carbon deposition for catalyst-M was increased from 27.6 to 37.1 at.% whereas for catalyst-B it was increased from 35.4 to 39.6 at.%. The increase in car-

Table 2
Percentage of carbon deposition on the catalyst surface at different stages of the reaction for catalysts- B, M and N

Catalyst	1 Day sulfidation (at.%)	2 Days sulfidation (at.%)	1 Day on stream (at.%)	5 Days on stream (at.%)	30 Days run (at.%)
B	22.6	28.3	35.4	39.6	44.1
M	21.7	21.6	27.6	37.1	36.4
N	18.5	19.1	22.7	29.6	28.2

Table 3
Ni dispersion obtained at different stages of the reaction for catalysts- B, M and N

Catalyst	A_{Ni2p}/A_{Al2p}				
	1 Day sulfidation	2 Days sulfidation	1 Day on stream	5 Days on stream	30 Days run
B	0.10	0.10	0.12	0.11	0.10
M	0.10	0.18	0.17	0.18	0.21
N	0.08	0.08	0.08	0.08	0.07

bon deposition for catalyst-M is probably due to the higher acidity of this catalyst. No significant change in carbon deposition was observed after 30 days of run time which indicates that the catalyst-M is comparatively stable with respect to catalyst-B.

The percentage of carbon deposition for catalyst-N (containing phosphorus) is also given in Table 2. In this case, no significant carbon deposition was observed after 2 days of sulfidation but the carbon deposition was increased from 19.1 to 22.7 at.% after 1 day on stream. After 5 days on stream the deposition was increased from 22.7 to 29.6 at.%, which was comparable with that on catalyst-M but higher than that on catalyst-B. No significant change in carbon deposition was observed after 30 days of run time, which also confirms that the catalyst containing phosphorus is also comparatively stable compared to catalyst-B.

From the above observation, it is concluded that the catalysts containing boron or phosphorus are comparatively more stable than catalyst without boron and phosphorus. It is necessary to note that, in addition to carbon, the adsorption of nitrogen compounds on the catalyst surface is also significantly responsible for possible catalyst deactivation. It was observed that there is no change in carbon deposition on these catalysts. But deactivation studies showed that the rate of deactivation for catalyst N was higher than those of catalysts-B and M with respect to the removal of total and basic nitrogen [20]. This indicates that not only carbon deposition but also nitrogen compounds adsorption on the catalyst surface plays an important role in deactivating the catalyst.

3.3.2. Ni dispersion

XPS results can be quantified for obtaining relative surface concentrations either by intensity or by peak area [38]. The ratio of peak area of A_{Mo3d}/A_{Al2p} and A_{Ni2p}/A_{Al2p} are usually used to study the dispersion of Mo and Ni on the support [39]). Mo and Ni are considered as the active and promoter metals, respectively, for hydrotreating reactions. The dispersion of these metals plays an important role on the activity of $NiMo/Al_2O_3$ catalyst.

The change in Ni dispersion at different stages of reactions is given in Table 3. From this table it is observed that the A_{Ni2p}/A_{Al2p} ratio improved after sulfidation. For example, the Ni/Al ratio for catalyst-B increased from 0.08 [$(Ni/Al)_{oxidic}$] to 0.10 upon 1 day of sulfidation and then remained unchanged throughout the reaction, suggesting that the dispersion remained unaffected by the time on stream and the extended period of time of reaction. This also indicates that the carbon deposition did not have any effect on Ni dispersion. A similar trend was also observed by Ozkan et al. [39]. In their work, the area ratio was unchanged after the catalysts were used in different reaction media. Ryan et al. [11] reported an increase in Ni dispersion upon sulfidation, whereas, Eijsbouts et al. [40] reported a decrease in Ni/Al ratio after sulfidation.

The A_{Ni2p}/A_{Al2p} ratio for catalyst-M increased significantly after sulfidation (see Table 3). For example, the A_{Ni2p}/A_{Al2p} ratio increased from 0.10 to 0.18 after 2 days of sulfidation. This ratio remained unchanged during period of stabilization and slightly increased with the increase in TOS. This result also suggests that boron greatly improved dispersion of Ni on the catalyst surface.

The A_{Ni2p}/A_{Al2p} ratio did not change for catalyst-N, and is comparatively lower than those obtained for catalysts-B and M, indicating that probably Ni is in a multilayer structure on catalyst-N. In the case of multilayer MoS_2 stacks, a Ni atom decorating the MoS_2 edges nearest to the alumina surface may be partly shadowed by the MoS_2 slabs on the top, which causes a decrease in Ni/Al ratio [41]. This result is in agreement with those obtained by Ryan et al. [11] and Eijsbouts et al. [40]. Ryan et al. [11] reported no change in Ni dispersion when P was added to $NiMo/Al_2O_3$ catalyst. Eijsbouts et al. [40] reported a slight decrease in the Ni/Al ratio upon sulfidation when 4 wt.% phosphorus to $NiMo/Al_2O_3$ catalyst. When 2 wt.% phosphorus was added, the decrease in the Ni/Al ratio was significant.

3.3.3. Mo dispersion

As suggested in the literature the ratio of A_{Mo3d}/A_{Al2p} can be used to illustrate the dispersion of Mo on the support [39]. This methodology was used in this work and the resulting dispersion of Mo on the catalyst surface is given in Table 4 for catalysts- B, N and M. The Mo/Al ratio in the oxidic catalyst was 0.33. From this Table it is observed that the Mo/Al ratio for catalyst-B improved to 0.5 after sulfidation indicating that sulfidation of $NiMo/Al_2O_3$ catalyst greatly improved the dispersion of this active metal. An increase in A_{Mo3d}/A_{Al2p} ratio upon sulfidation reveals a high dispersion of MoS_2. It was also observed from this table that the A_{Mo3d}/A_{Al2p} ratio increased upon precooking to 0.7 and even after 30 days of run time (to 0.82). It could be due to the redistribution of Ni and Mo on the catalyst surface at different stages of reactions which caused enrichment of Ni and Mo species on the catalyst surface [42]. Ozkan et al. [39] and Eijsbouts et al. [40]

Table 4
Mo Dispersion obtained at different stages of the reaction for catalysts- B, M and N

Catalyst	A_{Mo3d}/A_{Al2p}				
	1 Day sulfidation	2 Days sulfidation	1 Day on stream	5 Days on stream	30 Days run
B	0.50	0.50	0.63	0.70	0.82
M	0.67	1.1	1.4	1.6	1.6
N	0.40	0.40	0.34	0.32	0.43

also observed a significant improvement of A_{Mo3d}/A_{Al2p} ratio after sulfidation. Brito et al. [35] observed an increase in Mo/Al ratio after deactivation of the catalyst.

It was observed that the dispersion of Mo increased significantly with TOS due to the incorporation of boron in $NiMo/Al_2O_3$ catalyst (see Table 4). For, example the Mo dispersion increased from 0.33 to 0.67 after one day of sulfidation and increased significantly at every stage of the reaction. Mo dispersion of greater than 1 for catalyst-M indicates that the number of Al atoms on the catalyst surface is lower than the number of Mo atoms as the Mo dispersion is defined as A_{Mo3d}/A_{Al2p}. Decrease in Al atoms on the catalyst surface could be due to the partial coverage of alumina by B_2O_3. It is also known that boron affects the chemical states of Ni and Mo in the catalysts. For example, boron species prevent Ni and Mo from entering the lattice of alumina [43], which in turn causes an increase in surface Mo concentration.

The addition of phosphorus caused a slight decrease in Mo dispersion. No trend was observed with respect to Mo dispersion and time on stream (see Table 4). A slight improvement in dispersion was observed after 30 days of run time, which could be due to the slight rearrangement of Mo dispersion at different stages of reactions. The dispersion was significantly lower than that obtained from catalyst-M. From this observation it can be anticipated that Mo on the surface of catalyst-N is in multilayer MoS_2 stacks and in different sizes. The decrease in Mo dispersion indicates that some Mo atoms in the stack are shadowed by others and this was not identified by XPS analysis. This result is in agreement with those reported by Ryan et al. [11]. The above results indicate that sulfidation and precoking caused redistribution and enrichment of Mo and Ni on the catalyst surface. A similar conclusion was made by Li et al. [42].

3.3.4. Oxidation states

XPS analysis was also used to study the oxidation states of S, Ni and Mo as well as to identify different S, Ni and Mo compounds present on the catalyst surface. The detailed findings are described in the following sections.

3.3.4.1. Oxidation states of Mo. The summary of Mo 3d XPS results for catalysts- B, M and N at different stages of the reaction is given in Table 5. This shows two different oxidation states for Mo ions (Mo^{4+} and Mo^{6+}) and the corresponding binding energy (BE). The peak at 229.4 ± 0.2 eV is due to the presence of Mo^{4+} ions in the type of MoS_2 or MoO_2 [35,44–48]. The peak at 234.1 ± 0.2 eV is due to the presence of MoO_3 or $Al_2(MoO_4)_3$ [47–49]. It is evident that after two days of sulfidation the presence of Mo^{6+} is significantly lower in catalyst-M than those in catalysts- B and N, which indicates that boron reduces the interaction of Mo with the alumina support thus decreasing the formation of $Al_2(MoO_4)_3$. The percentage of Mo^{6+} and Mo^{4+} varies slightly at different stages of the reaction. However, from the Mo 3d spectra, it is difficult to detect the formation of the Ni–Mo–S structure, because the range of BE of Mo(IV) oxide and MoS_2 are similar (~229.4 eV) [50].

3.3.4.2. Oxidation states of Ni. Ni 2p spectra of catalysts- B, M and N were recorded. All catalysts showed a complex line profile of Ni^{2+} ion. The spectra was deconvoluted in three main components; one in the region of 853.1–854.5 eV, another in the region of 856.5–856.8 eV and a minor peak at ~862.1 eV. The oxidation states of Ni corresponding to two major peaks are listed in Table 6. The peak in the range of 853.5–854.5 eV contributes to the presence of Ni^{2+} in sulfided form. Ng and Hercules [51] reported the presence of Ni_3S_2 at the BE of 853.7 eV and Ni_2S at the BE of 854.0. On the other hand, Vradman and Landau [52] indicated the presence of Ni_3S_2 at the BE of 854.3. A peak at 856.5 eV is attributed to the presence of unsulfided Ni [53]. A peak at 862.1 eV is due to the shake up process of Ni–O [36,54] (this peak is not shown in Table 6).

Table 5
Oxidation states of Mo obtained at different stages of the reaction for catalysts- B, M and N

Catalyst	Binding energy (eV)	Oxidation state	1 Day sulfidation (at.%)	2 Days sulfidation (at.%)	1 Day on stream (at.%)	5 Days on stream (at.%)	30 days run (at.%)
B	229.4 ± 0.2	+4	84.8	88.8	85.3	86.4	77.0
	234.1 ± 0.2	+6	15.2	11.2	14.7	13.6	33.0
M	229.4 ± 0.2	+4	85.8	96.4	91.7	93.0	93.8
	234.1 ± 0.2	+6	14.2	3.6	8.3	7.0	6.2
N	229.4 ± 0.2	+4	83.0	88.4	91.3	88.9	91.2
	234.1 ± 0.2	+6	17.0	11.6	8.7	11.1	8.8

Table 6
Oxidation states of Ni obtained at different stages of the reaction for catalysts- B, M and N

Catalyst	Binding energy (eV)	Oxidation states	1 Day sulfidation (at.%)	2 Days sulfidation (at.%)	1 Day on stream (at.%)	5 Days on stream (at.%)	30 Days run (at.%)
B	853.5[a]	+1; +2; +4	22.4	36.4	37.8	45.5	50.0
	856.6[b]	+2	77.6	63.6	62.2	54.5	50.0
M	853.5[a]	+1; +2; +4	31.0	47.5	45.0	50.0	47.1
	856.6[b]	+2	69.0	52.5	55.0	50.0	52.9
N	853.5[a]	+1; +2; +4	29.6	30.8	33.3	32.0	44.0
	856.6[b]	+2	70.4	69.2	66.7	68.0	56.0

[a] Oxidation state: +1, due to the presence of Ni_2S; +2, due to the presence of NiS; and +4 due to the presence of Ni_3S_2.
[b] Oxidation state: +2, due to the presence of $NiAl_2O_4$.

Table 7
Oxidation states of sulfur obtained at different stages of the reaction for catalysts- B, M and N

Catalyst	Binding energy (eV)	Oxidation states	1 Day sulfidation (at.%)	2 Days sulfidation (at.%)	1 Day on stream (at.%)	5 Days on stream (at.%)	30 Days run (at.%)
B	162.5 ± 0.2	−2	59.5	68.8	67.4	66.7	68.9
	169.3 ± 0.2	+6	40.5	31.2	32.6	33.3	31.0
M	162.5 ± 0.2	−2	72.2	89.3	86.2	87.9	92.2
	169.3 ± 0.2	+6	27.8	10.7	13.8	12.1	7.8
N	162.5 ± 0.2	−2	43.7	67.9	70.3	73.7	75.6
	169.3 ± 0.2	+6	56.3	32.1	29.7	26.3	24.4

For catalyst-B, the concentration of sulfided Ni increased with the increase in time on stream (see Table 6). It is probably due to the deposition of Ni from feed to the catalyst surface as the sulfide form [53]. Table 6 also shows that significant amount of oxidic Ni is still present on the catalyst surface after 30 days of run time. Brito et al. [35] also reported significantly higher concentrations of oxidic Ni on the coked catalyst surface.

Similar oxidation states were also observed for catalysts- M and N. For these catalysts, the concentration of sulfided Ni increased after 2 days sulfidation and then changed slightly with the increase in time on stream (see Table 6).

From the above results, it was observed that after 2 days of sulfidation the formation of Ni sulfide for the catalyst containing boron (catalyst-M) is higher than those for catalysts- B and N, which indicates that boron increases the sulfidation of the catalyst.

3.3.4.3. Oxidation states of sulfur. The oxidation states of sulfur (OSS) at different stages of reactions were obtained from S 2p XPS spectra for catalysts- B, M and N. The results are summarized in Table 7 indicating that the oxidation states were −2 and +6. The higher the percentage of sulfur in the form of the oxidation state of −2, the higher the extent of sulfidation and hence catalyst activity. The peak at the binding energy (BE) of 162.5 ± 0.2 eV indicates the formation of Ni–Mo–S phase or NiS [39] due to OSS of −2, which is close to the value reported in the literature [35,38,39,50,53,55]. Another peak at a higher BE (169.3) was also observed. This peak at 169.3 ± 0.2 eV could be due to the presence of Ni_3S_2 [52] or oxidic sulfur species like SO_3^{2-} or SO_4^{2-} [35], which could be due to the presence of a relatively high amount of H_2S on the catalyst surface [56]. A similar peak was also observed by Callejas et al. [44,45,53,57]. This result agrees with that obtained from S K edge XANES.

From Table 7 it is observed that the formation of S^{2-} increased significantly for all three catalysts after two days of sulfidation. For example, it increased from 59.5 to 68.8 at.% for catalyst-B. Formation of S^{2-} for catalyst-B changed slightly with time on stream.

The presence of similar types (but different quantities) of S species is observed on catalysts- M and N. Table 7 shows that the quantity of S^{2-} species is significantly higher than that of S^{+6} species on catalyst-M, which indicates that boron enhances the sulfidation of $NiMo/Al_2O_3$ catalyst. The formation of S^{2-} increased from 72.2 to 89.3 % after two days of sulfidation and changed slightly with the TOS. Catalyst-N had less S^{2-} after one day of sulfidation than catalysts-B and M which could be due to the fact that catalyst-N had multilayer stacks of MoS_2 and therefore some sulfur atoms (underneath the top layer) will be shadowed. Cruz et al. [58] also reported lower S^{2-} species on the phosphorus containing catalyst (similar to catalyst-N). From the above observation, it can be concluded that sulfur in catalysts- B, M and N is present in the form of −2 and +6 oxidation states and the presence of boron enhances the sulfidation of the catalyst.

4. Conclusions

EXAFS analysis showed similar P–O bond distance in all catalyst samples. S K-edge XANES and XPS analyses confirmed the presence of sulfur in two oxidation states in sulfided $NiMo/Al_2O_3$ catalyst. Boron forms B_2O_3 on the catalyst surface whereas phosphorus caused the formation of PO_4 on the catalyst surface. Boron and phosphorus sig-

nificantly increased the sulfidity of the catalyst which was confirmed from XPS analysis. Ni and Mo dispersion also increased significantly with the incorporation of boron to $NiMo/Al_2O_3$ catalyst. Boron and phosphorus containing catalyst showed less carbon deposition on the catalyst surface than that from catalyst without boron and phosphorus. Ni was present on catalyst in the form NiS, Ni_3S_2, Ni_2S whereas Mo was present on the sulfided catalyst surface as MoS_2, MoO_2 and MoO_3. The at.% of sulfur in oxidation states of −2 and +6 did not change significantly with the increase in time on stream. However, the at.% of different Ni and Mo oxidation states changed somewhat with the change in time on stream.

Acknowledgements

The financial supports to A.K. Dalai from NSERC Collaborative Research and Development Grant and Syncrude Canada Ltd. and to D. Ferdous in the form of NSERC IPS 2 scholarship are acknowledged. The authors are also grateful to Synchrotron Radiation Centre (CRC), Madison, WI, for EXAFS and XANES and to Dr. L. S. Kotlyar at National Research Council, Ottawa for XPS analysis.

References

[1] P. Lulic, Oil Gas Europ. Magaz. 26 (2000) 33.
[2] H. Schweiger, P. Raybaud, H. Toulhoat, J. Catal. 212 (1) (2002) 33.
[3] H.R. Reinhoudt, R. Troost, A.D. van Langeveld, J.A.R. van Veen, S.T. Sie, J.A. Moulijn, J. Catal. 203 (2) (2001) 509.
[4] J.M.E. Hensen, J.P. Kooyman, V.D.Y. Meer, V.D.M.A. Kraan, H.J.V. De Beer, A.R.J. Van Veen, A.R. Van Santen, J. Catal. 199 (2001) 224.
[5] S. Kasztelan, Langmuir 6 (1990) 590.
[6] H. Toulhoat, S. Kasztelan, Proc. Int. Congr. Catal. 1 (9th) (1988) 152.
[7] S. Kasztelan, H. Toulhoat, J. Grimblot, P.J. Bonnelle, Appl. Catal. 13 (1984) 127.
[8] S.C. Fung, J. Catal. 58 (1979) 454.
[9] M. Houalla, B. Delmon, Surf. Inter. Anal. 3 (1981) 103.
[10] I. Alstrup, I. Chorkendorff, R. Candia, B. Clausen, H.J. Topsoe, J. Catal. 77 (2) (1982) 397.
[11] R.C. Ryan, R.A. Kemp, J.A. Smegal, D.R. Denley, G.E. Spinnler, Adv. Hydrotreat. Catal. 50 (1989) 21.
[12] S. Eijsbouts, V. Gruijthuijsen, J. Volmer, J.H.V.B. De, R. Prins, Adv. Hydro. Catal. 50 (1989) 79.
[13] W.F. Lytle, H.G. Via, H.J. Sinfelt, in: H. Winick, S. Diniach (Eds.), Synchrotron Radiation Research, Plenum Press, New York, 1980.
[14] R. Burch, A. Collins, Appl. Catal. 18 (1985) 389.
[15] J.A. Rodriguez, S. Chaturvedi, C.J. Hanson, A. Albornoz, J.L. Brito, J. Phys. Chem. B 103 (1999) 770.
[16] R. Cattaneo, T. Weber, T. Shido, R. Prins, J. Catal. 191 (2000) 225.
[17] R. Cattaneo, F. Rota, R. Prins, J. Catal. 199 (2) (2001) 318.
[18] I. Pettiti, I.L. Botto, C.I. Cabello, S. Colonna, M. Faticanti, G. Minelli, P. Porta, H.J. Thomas, Appl. Catal. A General 220 (1–2) (2001) 113.
[19] D. Ferdous, A.K. Dalai, J. Adjaye, Appl. Catal. 260 (2) (2004) 137.
[20] D. Ferdous, A.K. Dalai, J. Adjaye, Appl. Catal. 260 (2) (2004) 153.
[21] S. Eijsbouts, J.J.L. Heinerman, H.J.W. Elzerman, Appl. Catal. 105 (1993) 69.
[22] J. Rose, A.-M. Flank, A. Masion, J.-Y. Bottero, P. Elmerich, Langmuir 13 (1997) 1827.
[23] P.A. Hitchcock, C.D. Manvini, J. Electron. Spectrosc. 67 (1) (1994) 1.
[24] S. Chaturvedi, A.J. Rodriguez, J.L. Brito, Catal. Lett. 51 (1998) 85.
[25] M.E. Fleet, S. Muthupari, Am. Mineral. 85 (2000) 1009.
[26] M.E. Fleet, S. Muthupari, J. Non-Cryst. Solids 255 (1999) 233.
[27] M.E. Fleet, X. Liu, Phys. Chem. Minerals 28 (2001) 421.
[28] K. Peil, L.G. Galya, G. Marcelin, J. Catal. 115 (1989) 441.
[29] D. Li, T. Sato, M. Imamura, H. Shimada, A. Nishijima, J. Catal. 170 (1997) 357.
[30] R. Franke, J. Hormes, Physica 216 (1995) 85.
[31] N. Okude, H. Noro, M. Nagoshi, H. Yamamoto, Y. Baba, T.A. Sasaki, J. Elec. Spec. Rel. Phe. 88–91 (1998) 467.
[32] J.A. Rodriguez, J.-Y. Kim, J.C. Hanson, S.J. Sawhill, M.E. Bussell, J. Phys. Chem. B 107 (2003) 6276.
[33] M. Absi-Halabi, A. Stanislaus, D.L. Trimm, Appl. Catal. 72 (2) (1991) 193.
[34] H. Beuther, O.A. Larson, A.J. Perrotta, Studies Surf. Sci. Catal. 6 (1980) 271.
[35] A. Brito, R. Arvelo, A.R. Gonzalez, M.E. Borges, J.L.G. Fierro, Ind. Eng. Chem. Res. 37 (2) (1998) 374.
[36] L. Zhang, G. Karakas, U.S. Ozkan, J. Catal. 178 (1998) 457.
[37] M. Marafi, A. Stanislaus, Appl. Catal. A General 159 (1–2) (1997) 259.
[38] U.S. Ozkan, L. Zhang, S. Ni, E. Moctezuma, Energy Fuels 8 (4) (1994) 830.
[39] U.S. Ozkan, L. Zhang, S. Ni, E. Moctezuma, J. Catal. 148 (1) (1994) 181.
[40] S. Eijsbouts, J.N.M. Van Gestel, J.A.R. Van Veen, V.H.J. De Beer, R. Prins, J. Catal. 131 (1991) 412.
[41] S.M.A.M. Bouwens, F.B.M. Vanzon, M.P. Vandijk, A.M. Vanderkraan, V.H.J. Debeer, J.A.R. Vanveen, D.C. Koningsberger, J. Catal. 146 (1994) 375.
[42] D. Li, A. Nishijima, D.E. Morris, G.D. Guthrie, J. Catal. 188 (1999) 111.
[43] A.M. Stranick, M. Houalla, M.D. Hercules, J. Catal. 104 (1987) 396.
[44] J.F. Moulder, W.F. Stickle, P.E. Sobol, K.D. Bomben, Handbook of XPS, Perkin Elmer Corporation, Eden Prairie, MN, 1992.
[45] Z. Sarbak, S. Andersson, T. Lars, Appl. Catal. 69 (2) (1991) 235.
[46] J. Grimblot, P. Dufresne, L. Gengembre, J.P. Bonnelle, Bull. Soc. Chim. Bel. 90 (12) (1981) 1261.
[47] T. Okamoto, H. Nakano, T. Shimokawa, J. Catal. 50 (1977) 447.
[48] T.A. Patterson, J.C. Carver, D.E. Leyden, D.M. Hercules, J. Phy. Chem. 80 (16) (1976) 1700.
[49] A.V. Ramaswamy, L.D. Sharma, A. Singh, M.L. Singhal, S. Sivasanker, Appl. Catal. 13 (1985) 311.
[50] R. Hernández-Huesca, J. Mérida-Robles, P. Maireles-Torres, E. Rodríguez-Castellón, A. Jiménez-López, J. Catal. 203 (2001) 122.
[51] K.T. Ng, D.M. Hercules, J. Phy. Chem. 80 (19) (1976) 2094.
[52] L. Vradman, M.V. Landau, Catal. Lett. 77 (1–3) (2001) 47.
[53] M.A. Callejas, M.T. Martinez, J.L.G. Fierro, C. Rial, J.M. Jimenez-Mateos, F.J. Gomez-Garcia, Appl. Catal. A General 220 (1–2) (2001) 93.
[54] P.L. Arias, J.F. Canbra, M.B. Guemez, J.A. Legarreta, B. Pawelec, J.L.G. Fierro, Bull. Soc. Chim. Belg. 104 (4–5) (1995) 197.

[55] L. Salvati Jr., L.E. Makovsky, J.M. Stencel, F.R. Brown, D.M. Hercules, J. Phy. Chem. 85 (24) (1981) 3700.
[56] J. Cruz, M. Avalos-Borja, R.L. Cordero, M.A. Banares, J.L.G. Fierro, J.M. Palacios, A.L. Agudo, Appl. Catal. A General 224 (2002) 97.
[57] J.M. Jimenez-Mateos, J.M. Trejo, S. Vic, B. Pawelec, J.L.G. Fierro, Preprints—American chemical society, Div. Pet. Chem. 38 (1) (1993) 67.
[58] J. Cruz, M. Avalos-Borja, R.L. Cordero, M.A. Banares, J.L.G. Fierro, J.M. Palacios, A.L. Agudo, Appl. Catal. A General 224 (2002) 97.